Supplementary data: A Low-cost Paper-Based Platform for Fast and Reliable Screening of Cellular Interactions with Materials

E. Rosqvist[1] & E. Niemelä[2,7], J. Frisk[3], H. Öblom[4], R. Koppolu[5], H. Abdelkader[2,7], D. Soto Véliz[5], M. Mennillo[6], A. P. Venu[2,7], P. Ihalainen[1], M. Aubert[6], N. Sandler[4], C-E. Wilén[6], M. Toivakka[5], J. E. Eriksson[2,7], R. Österbacka[3], J. Peltonen[1]

[1]Laboratory of Physical Chemistry, Center for Functional Materials, Åbo Akademi University, Porthansgatan 3-5, 20500 Åbo, Finland

[2]Laboratory of Cell Biology, Center for Functional Materials, Åbo Akademi University, Bio City, Artillerigatan 6B, 20521 Åbo, Finland

[3]Laboratory of Physics, Center for Functional Materials, Åbo Akademi University, Porthansgatan 3-5, 20500 Åbo, Finland

[4]Pharmaceutical Sciences Laboratory, Åbo Akademi University, Artillerigatan 6A, 20520 Åbo, Finland

[5]Laboratory of Paper Coating, Center for Functional Materials, Åbo Akademi University, Porthansgatan 3-5, 20500 Åbo, Finland

[6]Laboratory of Polymer Technology, Center for Functional Materials, Åbo Akademi University, Biskopsgatan 3-5, 20500 Åbo, Finland

[7]Turku Bioscience Centre, University of Turku and Åbo Akademi University, 20520 Åbo, Finland

Keywords: *In vitro,* Printable, Cell culture, Screening platform, Drug testing, Material testing, Passive regulation,

Supplementary data.

Additional materials data. Studies was also conducted on a multi-layer curtain-coated barrier paper (referred to as MCP). The fabrication of the specialty paper has been described by Bollström et al. [1] In brief, a multilayer coating, with a top and bottom barrier layer, was applied to a wood-free pre-coated base paper. The main components of the barrier layers were latex and hyper-platy barrier kaolin. Surfactants and thickeners were used to adjust the surface tension and rheology of the coating to improve coatability. A smooth top surface was obtained by laboratory scale calendering with three nip passes at 120 kN/m and 70 °C.

The MCP was successfully coated with the given latex blends and PDMS for forming the well structures as described in the main text. While successful studies were conducted on this platform, the softness and thinness of the paper resulted in significant warping during tests in incubator conditions (data not shown). The warping could be counteracted by frame structures. This however, defeated the purpose of making an independent self-supported platform. In the appendices some additional data for the MCP are given for comparison.

Additional contact angle data

Table A – Full contact angle data, corrected for roughness, and the corresponding calculated determined with the OWRK method for the different substrates polydimethyl siloxane (PDMS), wax, the multi-layer curtain-coated barrier paper (MCP), the paperboard (BKS), the commercial latex blend (HPY83:HPC26) and the synthesized latex blends L01-L01 and L05-L02. Surface tension values of the probe liquids water, ethylene glycol (EG) and diiodo methane (DIM) were as suggested by van Oss, Chaudhury and Good. The contact angle values include the standard deviation.

Sample	Contact angle [°]			Surface Energy [mJ m^{-2}]		
	Water	EG	DIM	Dispersive	Polar	Total
PDMS[33,a]	114 ± 1	92 ± 2	96 ± 1	11.8	0.6	12.4
ColorQube Wax (black)	109 ± 1	85 ± 1	59 ± 1	29	0.0	29.0
MCP	84 ± 3	71 ± 2	68 ± 2	24.0	5.9	29.9
BKS	65 ± 2	64 ± 1	71 ± 4	22.3	17.3	39.6
HPY83:HPC26	77 ± 3	50 ± 3	53 ± 2	32.6	6.3	38.9
L01-L02	73 ± 1	73 ± 1	61 ± 3	28.0	9.8	37.8
L05-L02	73 ± 2	76 ± 1	61 ± 3	28.0	9.8	37.8

The MCP paper was determined to be less hydrophilic (water CA 84°) than the BKS paper (water CA 65°). In terms of surface energy the dispersive components were largely similar

of both paper substrates (24.0 mJ m^{-2} and 22.3 mJ m^{-2} respectively) but the polar contributions to the overall surface energy was much larger for the BKS paper, being 17.3 mJ m^{-2} compared to 5.9 mJ m^{-2} leading to a noteable larger surface energy for the BKS paper – 39.6 mJ m^{-2} compared to 29.9 mJ m^{-2}. Nonetheless, roll-to-roll coating of the latex blends was possible on the MCP.

Additional barrier properties

The uncoated base substrate MCP was an excellent barrier for the two test liquids: ethanol and vegetable oil, providing a barrier for the full 72 h (4260 min) of measurement. However, the barrier to deionized water was lowered to less than 90% (corresponding to 10% of the analyzed pixels showing signs of liquid penetration) after 1 h of interaction. Adding one coating layer of the synthesized latex blend was sufficient to create an effective barrier against deionized water for three days of interaction. In contrast to MCP,

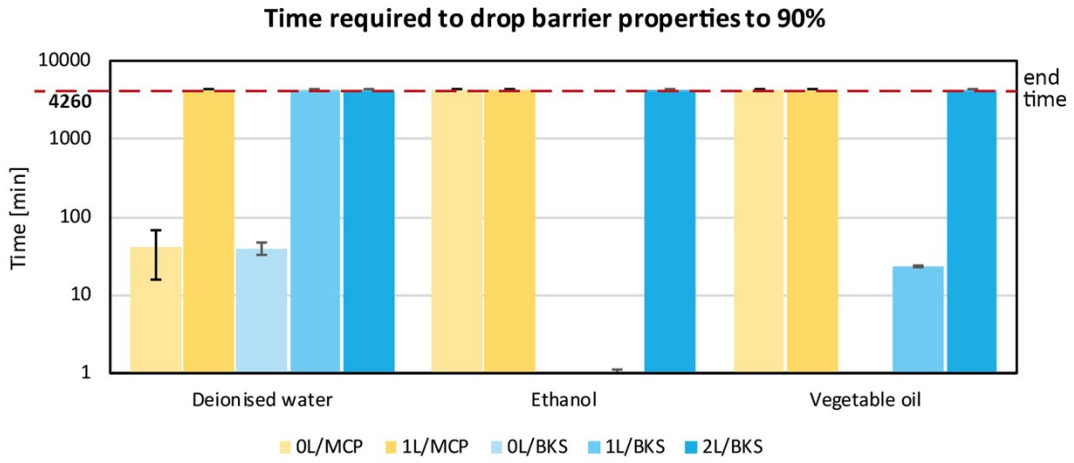

Figure 2. Time required to lose successful barrier properties. The substrates tested were MCP, and BKS in the variations: uncoated (0L), one layer of latex coating (1L), or two layers of latex coating (2L). The threshold set for defining sustained barrier properties was 90%, indicating a significant penetration of the solvent into the sample under that value. The maximum tested time of interaction (red line) was 4260 min (3 days) with the solvents deionised water, ethanol, and vegetable oil. The data represented is the average of three replicates with standard deviations.

Additional roughness data

Table B - Extended Table 4 of analysed roughness data, with summit densities (Sds), correlation lengths (Scl37) and normalised roughness (Sq/Scl37) added.

	S_q [nm]	S_{dr} [%]	S_{cl37} [nm]	S_q/S_{cl} [-]	S_{ds} [1/μm²]	S_{fd} [-]
MCP	42.1 ± 2.7	85.0 ± 6.4	99 ± 3	0.423	590 ±168	2.21± 0.01
BKS	52.8 ± 7.6	85.9 ± 16.6	117 ± 4	0.450	232 ± 41	2.18 ± 0.03
HPY83:HPC26 50:50	23.0 ±0.2	24.7 ± 0.9	83 ± 2	0.289	570 ± 65	2.22 ± 0.02
L01-L02 70:30	13.2 ± 0.2	1.9 ± 0.1	146 ± 18	0.092	610 ± 24	2.02 ± 0.03
L05-L02 70:30	3.3 ± 0.1	0.3 ± 0.01	173 ± 11	0.019	1955 ± 197	2.19 ± 0.01

All the latex coatings reduced the roughness of the base paper board significantly. The paper board had an initial roughness of 53 nm and 86%. Taking S_q as a measure of vertical roughness and S_{cl37} as a measure of horizontal roughness, the normalized roughness, S_q/S_{cl}, could be used to indicate the dominance of height variations over lateral variations in the topography. Of the used surface coatings, the normalized roughness was the lowest for the L05-L02, at 0.019, larger for L01-L02 and the largest for the commercial HPY83:HPC26 coating.

The density of summits, S_{ds}, was clearly the highest for the L05-L02 surface 1955 μm^{-2} in correspondence with it being a very smooth surface – the local maxima being very close to each other. The roughest substrate, the paper board, had in turn the lowest S_{ds}, 232 μm^{-2} as befits a surface with large structures and correspondingly large spacings between local maxima. The other investigated surfaces all had intermediate S_{ds} values within 570-610 $1/\mu m^2$.

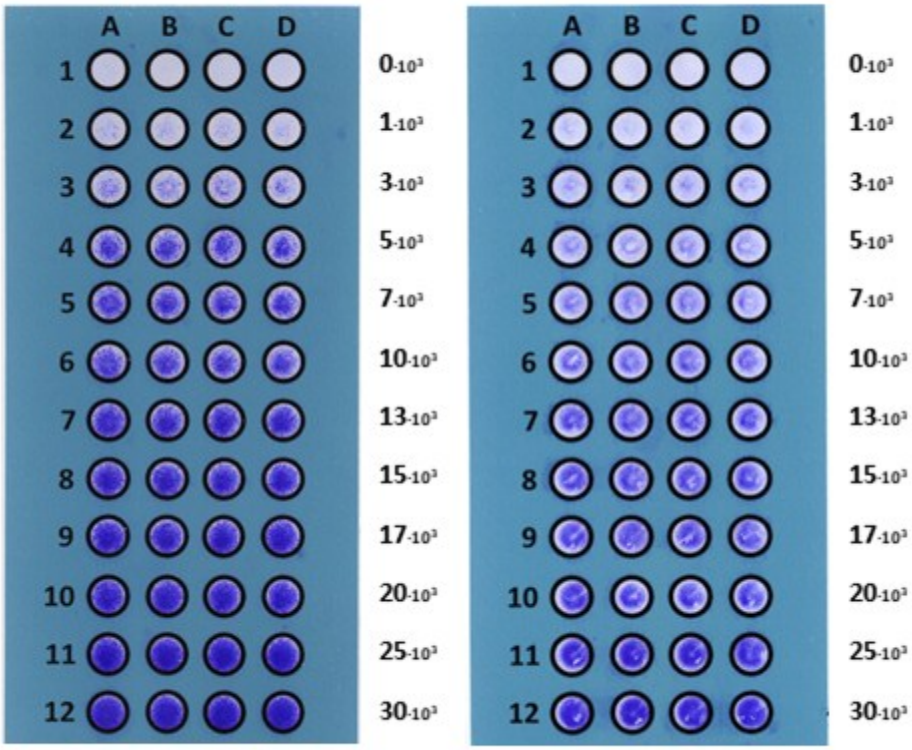

Supplementary Figure 1 - An used paper-based cell study platform with a nanostructured latex coating, and a wax-printed hydrophobic pattern surrounding 12 rows of 4 wells (A – D). In the wells an increasing number of HDF cells (left) and HeLa cells (right) have been grown for 24 h, and then stained with crystal violet.

A. Software Analysis.

Location and alignment of the assays. Multiple screening assays can be placed inside and captured by the document scanner to produce a single digital image, however, the assays may not overlap. The software recognizes the individual assays and analyses them separately. This feature can save a significant amount of manual work time for the user. This is possible due to the utilization of one-dimensional barcodes that aid in distinguishing the individual screening assays. First, the software locates barcodes in the scanner-produced digital image and extracts the assay regions of interest until no more can be located. An example of a sub image of such is shown in Figure 5. In addition to the barcodes, a triplet of high-contrast dots that aid in the alignment process are printed or made by coloring three wells with ink or a dye. These dots are automatically located after

the subimage extraction. The barcode contains information about the geometry parameters of the assay. These parameters are displayed in Figure 5. The geometry parameters define where in relation to the dot triplet the wells are located. Figure 1 also shows a successful location procedure of the two.

The standardized assay layout allows certain parameters of the geometry to be adjusted. The variables are; the dimensions of the array, the distance between wells, the well diameters, the axis lengths and the offset distance from the first well in the array to the origin of the coordinate system made up by the dot triplet, with separate values in the direction of either axis.

Analysis of the well contents. Assuming that the digital images of the paper platforms/substrates are produced using an ordinary color document scanner, the resulting digital images are likely represented in the tristimulus 'True color' color system, as arrays of pixels composed of red, green and blue (RGB) color components. The value of each component represented by 8 bits of data, resulting in 256 unique levels of intensity for each color component. By interpreting the RGB triplet as a simplified spectrum of light, we can study the absorption of light in the separate regions of the visible color spectrum.

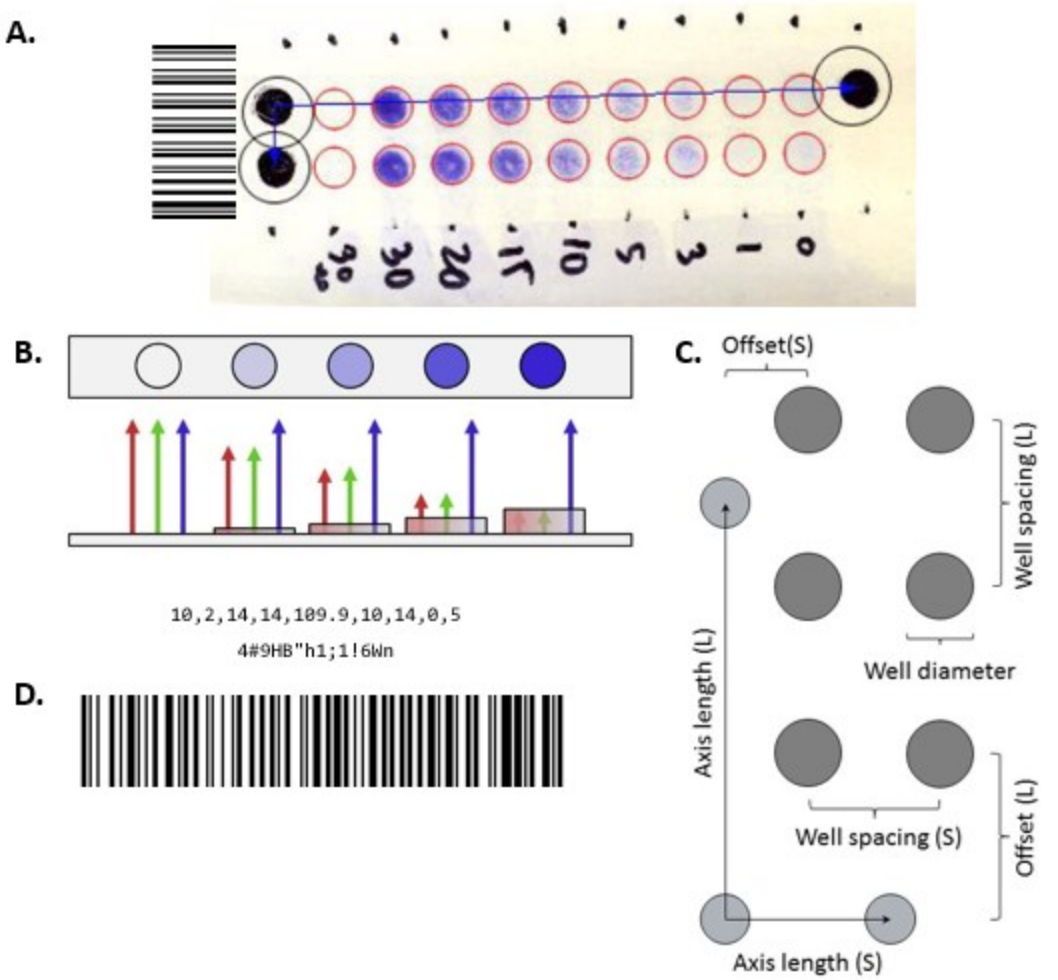

Supplementary Figure 2- Illustration of the software's working principle. A. Detection and alignment of wells, B. Principle of the software's color analysis in the wells, C. Well detection principle of the software and D. Barcode content description.

Dye. A dye can be used to colorize the cells in the wells. An increasing number of cells results in a more intense staining of a well. More staining yields a higher amount of absorption of the light hitting the platform surface. By measuring how much light is absorbed/reflected, the number of cells can be estimated. A blue dye will generally reflect blue wavelengths while absorbing red and green wavelengths of light. The correlation between red-green absorption and staining is visualized in Supp. Figure 2.

Quantification. Normalization of the data collected from the color component(s) of interest is possible by filling wells with both no cells and the minimum number of cells that result in maximum staining of the well. The intensity values of the array are then recalculated to make these values equal 0% and 100% respectively. The minimum number of cells that yields the maximum attainable staining could be found before conducting the experiment, in order to save wells. Wells with a higher number of wells will not give a correct intensity/staining value.

Cell Coverage. A user could also be interested in measuring the surface area of the well that is covered with cells. Wells with no cells can be selected and used as references. The highest staining intensities of these wells define a cut-off value for the background intensity. Staining intensities for pixels above this threshold are interpreted as cells. Dividing the number of pixels that are interpreted as cells by the total number of pixels of the well gives an estimate of the coverage ratio. A limitation to this method is that the background staining needs to be very consistent.

Post processing. The program exports the calculated data as delimiter-separated values in text files compatible with common data analysis software (e.g. Excel, Origin, MATLAB) for further processing. These files contain the calculated staining values and intensity histograms of each well and the cell coverage ratios if reference wells were selected in the program. After location of the assays, the background-separated wells can be automatically exported as individual images to be analyzed with other image analysis software. An option to export the raw data of each well is also available.

Barcode encoding. The information stored in the barcodes is an arbitrarily long series of integer or decimal numbers separated by a comma. The decimal point is represented by a period character. Thus, the data is a string of characters with 12 unique values minimum. The order of the numbers is as follows: number of wells along longitudinal direction (L), number of wells along transverse direction (S), well spacing (L), well spacing (S), axis length (L), axis length (S), offset (L), offset (S) and the well diameters, all in the same unit of measurement. The format used for the barcodes is Code-128, containing a string of

characters with 95 unique values each. Supp. Figure 2 shows an example of geometry parameters, the encoded counterpart shown as ASCII characters and the equivalent Code-128 format barcode. The barcode is to be printed with a height of 2 cm. This is needed for the software to extract the region of interest correctly. The size of the screening assay region is determined using the height and center position of the barcode along with the assay geometry information contained in the barcode. The orientation of the barcode dictates on which of its sides the well array is located.

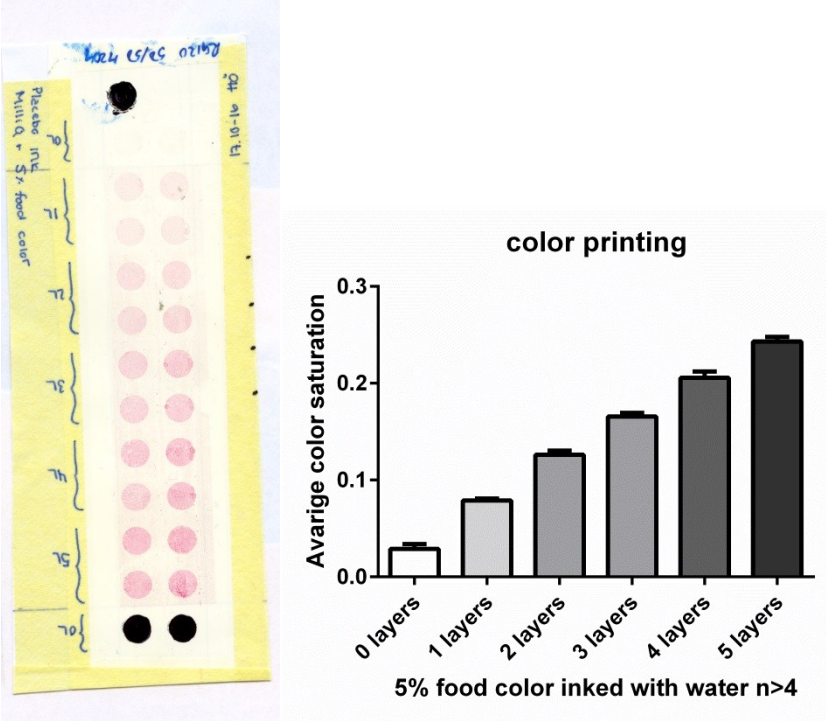

Supplementary Figure 3. Increasing layers of placebo ink containing 5% food color dissolved in water printed on paper strips in the preliminary study (n=4).

Drug concentration data. The layered DOX that dissolves over 24 h into phosphate-buffered saline solution (PBS) was studied to determine the drug loading of the inkjet-printed samples; an optically clear liquid with similar osmotic pressure as the cell medium was used. To compare the dissolved DOX, a standard DOX solution was prepared with the following final concentrations: 0 μg ml^{-1}, 0.01 μg ml^{-1}, 0.05 μg ml^{-1}, 0.1 μg ml^{-1}, 0.25 μg ml^{-1}, 0.5 μg ml^{-1}, 1 μg ml^{-1}, 5 μg ml^{-1}. The samples were transferred to a 96 well plate and analyzed with a Hidex Sense Beta Plus microplate reader using 485nm excitation and emission at 535 nm. To visually inspect the dispersion of the drug in the wells, dried DOX was scanned and analyzed or imaged.

References

[1] R. Bollström, M. Tuominen, A. Määttänen, J. Peltonen and M. Toivakka, "Top layer coatability on barrier coatings," *Progress in Organic Coatings,* vol. 73, no. 1, pp. 26-32, 2012.